

# IMPROVING THE PERFORMANCE OF HYPERSPECTRAL PUSHBROOM IMAGING SPECTROMETERS FOR SPECIFIC SCIENCE APPLICATIONS

F. Dell'Endice<sup>a,\*</sup>

<sup>a</sup> Remote Sensing Laboratories, Department of Geography  
University of Zurich – Winterthurerstrasse, 190 – 8057 Zurich - Switzerland  
francesco.dellendice@geo.uzh.ch

Commission WG VII/3

**KEY WORDS:** Hyperspectral, Spectral Binning, CCD, Pushbroom

## ABSTRACT:

Hyperspectral imaging spectrometers offer the unique chance of recording image data of a broad range of targets in the reflected solar energy spectrum. These instruments are designed upon certain requirements such as signal-to-noise ratio (SNR), spectral resolution and bandwidth or noise equivalent delta radiance. These parameters are determined by investigating one or several typical targets (e.g. vegetation, limnology, soil, atmosphere) that the instrument will sense during its operational life by means of specific instrument models.

Depending on the specific application, users can demand hyperspectral image data that might cover a portion or the whole sensor spectral range and, more importantly, may have requirements different from the ones the instrument was designed for originally. Therefore, in order to meet the user requests the spectrometer settings should be modifiable.

Many instruments are potentially programmable from the electric point of view, in a way that the sensor setting parameters could be changed, e.g. **exposure time, on-chip averaging, the so-called binning, amplifier gains**. By tuning these parameters the sensor performances can be modified according to the user needs.

The **Airborne Prism Experiment (APEX)**<sup>1</sup>, a hyperspectral imaging spectrometer developed by a Swiss-Belgium consortium on behalf of the European Space Agency (ESA) and under the scientific supervision of the Remote Sensing Laboratories (RSL), has been designed upon certain requirements (e.g. radiance levels, SNR) but, nevertheless, the electric settings can be changed by means of a mission control file in order to fulfil user requests that differ from the default scenario. Namely, the APEX instrument allows changes of **exposure time, on-chip binning and frame period**.

We designed and implemented a software utility that optimizes the instrument parameters based on the possible range of hardware settings and the user application requirements. This utility is based on the detector electrical and optical description, which is modelled in terms of signal and noise by using the SNR equation<sup>2</sup>. In order to develop such a model the instrument optical characteristics, i.e. transmission, must be known. The utility can be regarded as an APEX sensor simulator but it can be easily adapted to any other hyperspectral imaging apparatus.

Users (i.e. sensor manufacturers, operators, scientists) can formalize their requirements and feed them into the model. E.g. a scientist is aiming at estimating the amount of leaf chlorophyll content within a vegetation target with a required minimum of detectable differences. Therefore he has to identify the needed values of SNR, spectral resolution and sampling interval as an input for the simulator.

The utility evaluates all the possible solutions in terms of exposure time and on-chip binning in order to determine the one that matches the scientist needs the best. A broad variety of error deviations are reported in order to help the users in interpreting the simulation results, estimate the error and accuracy budgets accordingly.

Depending on the input requirements the discordance between the users needs and the results can be significant. In such a case the utility performs a further step by analyzing post-processing strategies, as for instance off-chip binning, in a way that the requirements can be somehow be met.

The presented utility has a twofold advantage: (1) it allows manufacturers and sensor operators to offer an instrument that is adaptable to needs of the end-users community and (2) it lets users, mainly scientists, understand what can be achieved with a given hyperspectral instrument. The weakness of the utility relies on the lack of information about the optical and electrical parameters, which might be caused by the confidential nature of technical details, namely in private companies.

We firmly believe that this utility can (a) optimize the programming of hyperspectral imaging spectrometers to gather more accurate image data and (b) let users exploit the broad range of applications that can be investigated with the available large spectral range.

---

\* Corresponding author.

## 1. INTRODUCTION

Hyperspectral imaging pushbroom spectrometers<sup>1,3,4</sup> are currently used in several domains in order to identify the spectral signatures of a broad range of materials in the reflected solar energy spectrum. Those instruments are designed such that they could sense the largest variety of targets with relatively high performances. Scientific requirements are retrieved by investigating the properties of representative applications (e.g. agriculture, limnology, vegetation, soil, atmosphere)<sup>5</sup> that the instrument will be used for along its operation life and they are formulated, for instance, in terms of required spectral resolution<sup>6,7</sup>, signal-to-noise ratio (*SNR*), noise-equivalent delta radiance (*NeΔL*)<sup>5</sup>, or spatial resolution. Such an approach is justified by the fact that both airborne and spaceborne sensors usually sense various targets at the same time, and reasonable instrument performances must be granted more or less all over the spectral range. Therefore every instrument comes with a default optical and electrical configuration.

Nevertheless scientists might be interested in a specific application that groups few similar targets and/or only a portion of the instrument spectral range; they could then request to optimize the instrument performances in that range. For instance, a scientist might want to discriminate 0.5% water content in an olive crop and he is interested in the spectral region between 300 and 800 nm. This specific application would generate new requirements that might be different from the ones upon the instrument has been designed on.

Certain instruments permit some of their electrical (e.g. gains, integration time) and/or optical parameters (e.g. filters) to be easily modified. Special devices can change the default configuration as, for instance, field programmable gate array (FPGA) cards; few lines of code are updated before a mission starts. Such a technique can be used for both airborne missions and spaceborne missions.

The instrument variables that can be changed are (1) the integration time (or exposure time), (2) the frame period, and (3) the spectral on-chip binning (also called spectral on-chip averaging). Those parameters can be set in a way that the instrument can meet, whether it is possible, the new requirements dictated from the specific science application.

Generally, the binning operation consists of summing lines up in a way that *SNR* can improve. The next sections (1) will explain further the tuning variable and (2) will show how an instrument configuration, being driven from a particular application, is generated.

## 2. PROBLEM MODELING

Scientists could require a hyperspectral sensor to flight for a specific application; it could then happen that the nominal instrument configuration is inadequate to such a purpose and must be modified in order to satisfy the scientific requirements of that particular application. An optimization tool is hereafter described.

Generally, those spectrometers provide data under the form of hyperspectral cubes<sup>8</sup>. Such a cube has two spatial dimensions, i.e. the across-track dimension and the along-track dimension (provided by the motion of the platform), and one spectral dimension, representing the spectral signature of every spatial pixel. A hyperspectral cube with *M* across-track pixels, *L* along-track pixels, and *P* spectral bands is here considered. The plane formed by the across-track and the spectral dimensions is called

frame; a frame has *M* spatial pixels (*M* columns) and *P* spectral pixels (*P* rows). **Figure 1** shows how the sensor generates such a cube.

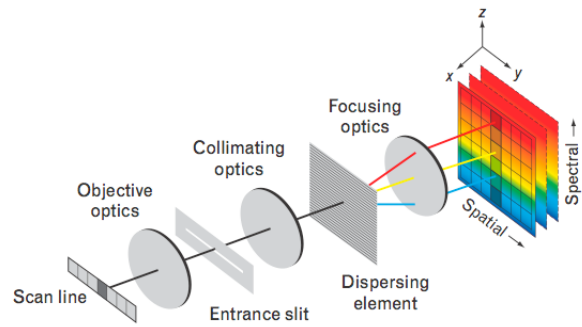


Figure 1: Optical chain of a common hyperspectral pushbroom spectrometer.

The model generates the application-driven sensor configurations by optimizing those two variables:

- **Integration time:** the interval of time used to collect photons of light on a detector. The higher the integration time, the higher is the signal.
- **Spectral Binning** (or spectral averaging or spectral zone mode): two or more spectral bands are summed up in a way that they form a unique row channel (**Figure 2**). If this summation is done by the hardware during image acquisition then is called *on-chip binning*, otherwise if it is performed offline by means of post processing algorithms is then called *off-chip binning*. In general, the higher the number of binned rows (bands), the higher is the spectral *SNR*.

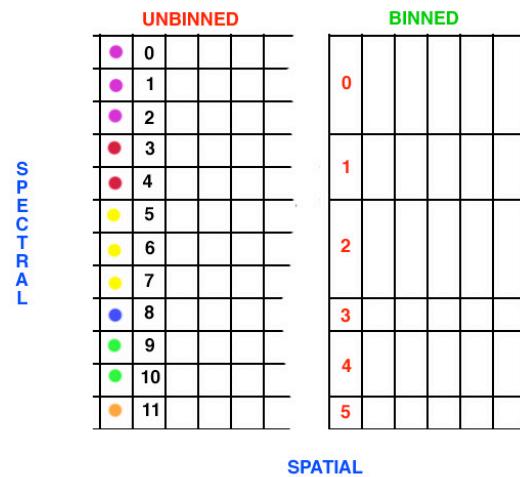


Figure 2: Spectral Binning. The number of across-track spatial pixels is preserved whereas the bands (0,1,2) are binned to form band (0), bands (3,4) will form band 1 and so on.

*Spatial binning* in the along-track and/or across-track direction can be also applied. We assume that the *M* x *L* x *P* cube dimensions refer to a sensor operated in the unbinned configuration; therefore the *M* x *P* size of the frame would most likely correspond to the one of the detector. The main detector architectures taken here in account are:

- A Charge Coupled Device (CCD).
- A Complementary Metal Oxide Semiconductor (CMOS).

It is apparent that any spectral binning will reduce the number of bands. The instrument is delivered usually with a default spectral binning pattern, defined upon the general mission requirements; frames are  $M \times B$  matrixes, where  $B \leq P$ . An instrument model based on the following variables is introduced:

- Noise sources (i.e. dark noise, amplifier noise, read-out noise, photon noise)
- Transmission of optics and chip quantum efficiency.
- Unbinned configuration of the chip (i.e. CCD or CMOS) in terms of both bandwidth and corresponding center wavelength.
- Other parameters (i.e. flight altitude, field-of-view (FOV)).

Those variables are grouped within a typical SNR equation that will be later on subjected to an optimization process.

The approximated signal equation is:

Equation 1: Signal equation.

$$S \propto F * \frac{L * A * 4 * \tan^2(FOV/2) * \tau * T * \lambda * \eta * S}{hc * N_e^{-2}}$$

where:

- L is the radiance.
- A is the instrument aperture.
- FOV is the Field Of View.
- T is the integration time.
- S is the spectral sampling interval, related to the FWHM.
- h is the Planck constant.
- c is the speed of the light.
- $N_e^-$  is the number of collected electrons.
- $\tau$  is the optical transmission.
- $\lambda$  is the center wavelength.
- $\eta$  is the detector quantum efficiency.
- F is the filter efficiency (if any).

It is apparent that the integration time as well as the binning pattern can increase the signal level and then the SNR performances by acting directly on the variables  $T$  and  $S$ .

The logic scheme behind the optimization tool is shown in Figure 3. Scientific requirements (on the extreme left) are the input for the instrument model based on the SNR equation; therefore the optimization algorithm will suggest how to configure the instrument in terms of integration time and binning pattern.

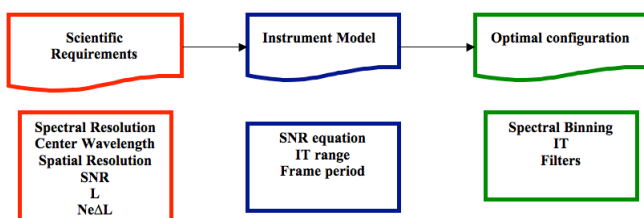


Figure 3: Software logical model.

The spectral binning is usually applied to CCD detectors, mostly adopted for the sensing in the visible or near infrared; the read out process can be in fact adjusted in a way that group of lines are summed up and read out at once.

CMOS detectors, mainly used in the short wavelengths domain, have a different reading architecture where every pixel is read independently from any other one; therefore on-chip spectral binning cannot be applied easily. Nevertheless off-chip binning can be applied.

Whenever a requirement cannot be met for any combination of unbinned spectral pixels then backup solutions must be adopted. The easiest one would be to relax the requirement until the performance is met. If the requirement is not met because of saturation then an *ad-hoc* filter could be design.

Theoretically, the ideal result of such an optimization would be the narrowest bandwidth with the highest SNR. The narrower is the bandwidth, and the finest are the spectral details that can be distinguished. Case studies are presented in next section.

### 3. CASE STUDIES

The model has been applied to different scenarios, each one coming with its own requirements. The case studies are the following:

- Sensor default configuration*: the instrument is tuned in a way that the largest variety of targets can be sensed with very high performances.
- Application driven*: requirements are generated by considering a typical vegetation application, and the spectral binning pattern is generated accordingly.

Results are shown mainly through tables; the subscript  $R$  stands for requirements while the  $C$  stands for calculated.

#### 3.1 APEX requirements

APEX<sup>1</sup>, the ESA Airborne Prism Experiment is a flexible hyperspectral mission simulator and calibrator for existing and upcoming or planned future space mission. Operating between 380 nm and 2500 nm in 300 freely configurable bands (up to 508 bands in full spectral mode), the system offers a 28° FOV and 1000 spatial pixels.

Variable frame rates and integration times allow adjusting for specific flying heights, speeds and patterns. The choice of predefined or user defined programmable binning patterns is offered and will be driven by the specific application and SNR needs.

The general APEX requirements for a medium radiance level are illustrated in Table 1, indicated by the variables with the subscript  $R$ .

The results of the simulations are shown in Table 1 whereas the final binning pattern is described in Table 2; the model results are indicated by the variables with the  $c$  subscript. The center wavelength requirements are all met with a very high accuracy as in shown in column 2. Thanks to high number of unbinned spectral bands the instrument is able to ensure most of the requirements with a spectral resolution less or equal than the required one. The performances are not satisfying at 780, 850 and 1000 nm. The requirements at 780 and 850 can be met only if a dedicated filter is designed at such wavelengths; the instrument would need to attenuate of 20% and 39% the signal respectively at 780 nm and 850 nm (the filter absorptivity is shown in Figure 4); it does mean that, even if the SNR requirement is met, the noise-equivalent-delta-radiance is not, therefore decreasing the resolution in distinguish between small quantities of chemical components into the targets. The requirement at 1000 nm is not met at all and it's because we

approach here the end of the detector where the quantum efficiency is very low; the model is very constrained here and adding additional spectral lines would mean only to generate a very high error in the center wavelength of this band.

Table 1: Requirements and Results for APEX Median Radiance requirements.

$\lambda_R$ [nm]	$\lambda_C$ [nm]	SSI <sub>R</sub> [nm]	SSI <sub>C</sub> [nm]	GSD <sub>R</sub> [m]	GSD <sub>C</sub> [m]
380	<b>387.73</b>	15	<b>16.30</b>	3.65	<b>3.65</b>
400	<b>400.55</b>	15	<b>8.80</b>	3.65	<b>3.65</b>
470	<b>469.85</b>	10	<b>8.97</b>	3.65	<b>3.65</b>
500	<b>500.53</b>	10	<b>9.92</b>	3.65	<b>3.65</b>
515	<b>515.59</b>	9	<b>9.59</b>	3.65	<b>3.65</b>
580	<b>581.77</b>	5	<b>4.06</b>	3.65	<b>3.65</b>
650	<b>650.89</b>	5	<b>2.86</b>	3.65	<b>3.65</b>
700	<b>698.83</b>	5	<b>3.51</b>	3.65	<b>3.65</b>
750	<b>749.61</b>	5	<b>4.27</b>	3.65	<b>3.65</b>
780	<b>781.45</b>	5	<b>4.76</b>	3.65	<b>3.65</b>
850	<b>850.98</b>	10	<b>5.89</b>	3.65	<b>3.65</b>
900	<b>901.81</b>	10	<b>6.73</b>	3.65	<b>3.65</b>
940	<b>937.16</b>	10	<b>7.30</b>	3.65	<b>3.65</b>
980	<b>983.54</b>	10	<b>8.04</b>	3.65	<b>3.65</b>
1000	<b>1000</b>	10	<b>8.29</b>	3.65	<b>3.65</b>

$\lambda_R$ [nm]	SNR <sub>R</sub>	SNR <sub>C</sub>	Ne $\Delta$ <sub>L<sub>R</sub></sub>	Ne $\Delta$ <sub>L<sub>C</sub></sub>	F
380	314	<b>716.35</b>	2.23e-4	<b>0.98e-4</b>	-
400	681	<b>692.27</b>	1.32e-4	<b>1.30e-4</b>	-
470	484	<b>924.07</b>	2.41e-4	<b>1.27e-4</b>	-
500	737	<b>897.31</b>	1.44e-4	<b>1.18e-4</b>	-
515	901	<b>879.91</b>	1.14e-4	<b>1.17e-4</b>	-
580	554	<b>557.14</b>	1.69e-4	<b>1.68e-4</b>	-
650	436	<b>444.64</b>	1.87e-4	<b>1.83e-4</b>	-
700	313	<b>450.99</b>	2.19e-4	<b>1.52e-4</b>	-
750	197	<b>604.96</b>	4.98e-4	<b>1.63e-4</b>	-
780	186	<b>623.29</b>	6.44e-4	<b>1.54e-4</b>	<b>0.80</b>
850	134	<b>629.56</b>	1.21e-3	<b>1.57e-4</b>	<b>0.61</b>
900	138	<b>590.81</b>	8.56e-4	<b>1.99e-4</b>	-
940	118	<b>239.08</b>	3.12e-4	<b>1.54e-4</b>	-
980	156	<b>176.11</b>	5.38e-4	<b>4.75e-4</b>	-
1000	121	<b>78.89</b>	6.53e-4	<b>1.01e-3</b>	-

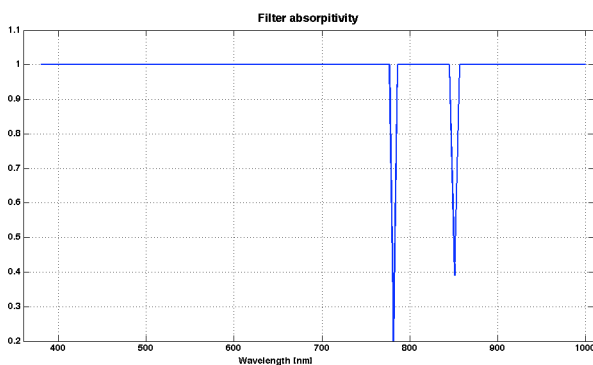


Figure 4: Customized filter for APEX Median Radiance Requirements.

Nevertheless 80% of the requirements have been met before applying any filtering solution. The **Figure 5** reports the error budget for every requirements; a very positive error means that the requirement has been satisfied and, on the other side,

implies that the instrument has the potentiality of performing much better than what requested. This is clearly a great advantage especially in terms of SNR and noise-equivalent-delta-radiance because it will allow (a) to detect a signal much higher than its corresponding noise and (b) to distinguish between radiance levels that might differ only for a few percent of chemical contents.

Table 2: Binning pattern for the APEX Median Radiance requirements.

R	1	2	3	4	5	6	7	8
First	1	35	132	160	172	214	243	258
Last	34	50	140	167	178	215	243	258
R	9	10	11	12	13	14	15	
First	271	278	291	299	304	310	312	
Last	271	278	291	299	304	310	312	

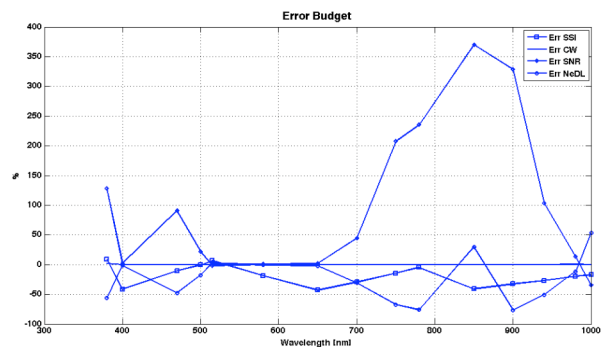


Figure 5: Error Budget For APEX Median Radiance Requirements.

### 3.2 Dedicated science application: Chlorophyll/Red-Edge

The optimization algorithm can be applied to specific science application and this case study illustrates how this is possible. Let's assume that it is necessary to identify the chlorophyll content within leaves with an accuracy of 2%, in the visible-near-infrared spectral region. A few reflectance canopy profiles of leaves with a content of chlorophyll between 10% and 80% are shown in **Figure 6**. (The PROSPECT<sup>9</sup> model has been used in order to generate reflectance curves in step of 2% chlorophyll content). When a leaf has more than 60% in chlorophyll content is very hard to distinguish the variations in reflectance because of the high absorption; therefore only curves up to 60% of chlorophyll have been considered.

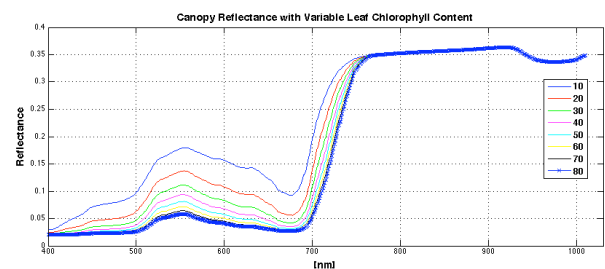


Figure 6: Canopy Reflectances with variable Leaf Chlorophyll Content. The content is indicated in microgramm/cm<sup>2</sup>.



The reflectance curves have been transformed into at-sensor radiance by using MOD0<sup>10</sup>, the graphical user interface to MODTRAN<sup>10</sup>.

A median radiance level is retrieved by averaging the highest curve (20% chlorophyll) with the lowest curve (i.e. 60% chlorophyll).

In order to run the model, it's necessary to derive the application driven requirements in terms of center wavelength, radiance, SNR, spectral resolution and noise-equivalent delta radiance. Bands are defined by considering the most interesting parts of the reflectance curves in **Figure 6**; the most demanding portion of the curve is the one corresponding to the red edge (i.e. between 680 nm and 750 nm). Therefore 4 bands are taken here each one with a spectral resolution of 5 nm in order to detect the slope of the red edge. Other 6 bands are considered before and after the red edge with a spectral resolution of about 10 nm.

Table 3: Vegetation (Chlorophyll Content - Red Edge) requirements.

$\lambda_R$ [nm]	$\lambda_C$ [nm]	SSIR [nm]	SSIC [nm]	GSD <sub>R</sub> [m]	GSD <sub>C</sub> [m]
400.2	<b>405.1</b>	10	<b>10.35</b>	3.65	<b>3.65</b>
450.4	<b>445.8</b>	10	<b>9.89</b>	3.65	<b>3.65</b>
499.9	<b>504.3</b>	10	<b>10.18</b>	3.65	<b>3.65</b>
550.9	<b>552.6</b>	5	<b>5.17</b>	3.65	<b>3.65</b>
559.9	<b>603.4</b>	10	<b>9.10</b>	3.65	<b>3.65</b>
650.9	<b>650.9</b>	5	<b>2.86</b>	3.65	<b>3.65</b>
681.7	<b>681.7</b>	5	<b>3.28</b>	3.65	<b>3.65</b>
702.4	<b>702.4</b>	5	<b>3.57</b>	3.65	<b>3.65</b>
728.9	<b>728.9</b>	5	<b>3.96</b>	3.65	<b>3.65</b>
749.6	<b>749.6</b>	5	<b>4.27</b>	3.65	<b>3.65</b>

$\lambda_R$ [nm]	SNR <sub>R</sub>	SNR <sub>C</sub>	Ne $\Delta$ <sub>R</sub>	Ne $\Delta$ <sub>C</sub>	F
400.2	404	<b>745</b>	1e-4	<b>6.7e-5</b>	-
450.4	70	<b>931</b>	8e-4	<b>6.0e-5</b>	-
499.9	45	<b>831</b>	11e-3	<b>5.9e-5</b>	-
550.9	37	<b>578</b>	18e-3	<b>1.1e-4</b>	-
559.9	31	<b>803</b>	16e-3	<b>6.0e-5</b>	-
650.9	30	<b>403</b>	12e-3	<b>8.7e-5</b>	-
681.7	31	<b>399</b>	10e-3	<b>7.6e-5</b>	-
702.4	29	<b>414</b>	16e-3	<b>1.2e-4</b>	-
728.9	84	<b>483</b>	7e-4	<b>1.2e-4</b>	-
749.6	551	<b>552</b>	2e-4	<b>1.9e-4</b>	-

The radiance requirement is defined by averaging the maximum radiance curve with the minimum radiance curve. The minimal difference of chlorophyll the scientist is interested in is 2%; this corresponds to the noise equivalent delta radiance (Ne $\Delta$ L), that is, the difference in radiance between two radiance curves, which differ for 2% chlorophyll content. Finally, we could define the SNR requirement by calculating the ratio between the medium radiance level and the Ne $\Delta$ L. The requirements are shown in **Table 3: Vegetation (Chlorophyll Content - Red Edge) requirements**.

The results of the simulations are shown in Table 4, and represented by the variables with the *c* subscript. It is apparent how all the requirements have been met with a tolerance of about 5% in all cases. The SNR makes an exception; in fact all the model SNR results are much higher than what requested. It does imply that the Ne $\Delta$ L is actually one order of magnitude smaller than the requirement. In other words, within the limits of the applicability of a linear assumption, that this instrument is

potentially able to distinguish chlorophyll content with an accuracy of better than 0.2 %.

The binning pattern for such an application is shown in **Table 4**.

Table 4: Binning pattern for the chlorophyll/red-edge application.

R	1	2	3	4	5	6	7	8	9	10
First	42	104	163	198	223	243	253	259	266	271
Last	59	115	170	200	226	243	253	259	266	271

#### 4. CONCLUSIONS

Specific scientific requirements might differ from the ones a hyperspectral pushbroom spectrometer has been designed with. An optimization algorithm is here presented. Such a model is based on both the SNR equation and the basic instrument electrical and optical parameters. The main goal of model is to provide a sensor configuration in terms of integration time and binning patterns in order to let the sensor meet the specific application requirements. Additional solutions are also discussed whether the instrument variables cannot be optimally tuned. Two case studies are therefore presented. In the first one a generic scenario has been used to define the default instrument requirements in terms of spectral and radiometric parameters and the corresponding nominal sensor setup is defined; a few requirements can be met only if a special filter is used. The second case study deals with a scientific application, that is, the identification of at least 2% differences in chlorophyll content within the optical signal generated by canopy. Results, errors, and binning patterns have been presented.

This optimization tool can be easily adapted to any sensor and independently from any kind of platform (i.e. airborne and spaceborne). Its main advantage consists of using as good as possible the programmability functionalities of current hyperspectral systems.

#### References from Journals:

1. J. Nieke, K.I. Itten, W. Debruyne, and the APEX team, "The Airborne Imaging Spectrometer APEX: from concept to realization," in Proceedings of 4<sup>th</sup> EARSel Workshop on Imaging Spectroscopy, Warsaw (2005)
2. J. Nieke, M. Solbring, and A. Neumann, "Noise contributions for imaging spectrometers," in Applied Optics, Vol.38 No. 24 (1999)
3. I. Baarstad, T. Løke, and P. Kaspersen, "ASI - A new airborne hyperspectral imager," in Proceedings of the 4<sup>th</sup> EARSel Workshop on Imaging Spectroscopy - New Quality in Environmental Studies, Warsaw, Poland (2005)
4. C. O. Davis, J. Bowles, R. A. Leathers, D. Korwan, et al., "Ocean PHILLS hyperspectral imager: design, characterization, and calibration," in Optic Express, Vol. 10, No. 4 (2002)
5. D. Schlöpfer and M. Schaepman, "Modelling the noise equivalent radiance requirements of imaging spectrometers based on scientific applications," in Applied Optics, OSA41(27):5691-5701.
6. R. O. Green, "Spectral calibration requirement for Earth-looking imaging spectrometers in the solar-reflected spectrum," in Applied Optics, Vol. 37 No.4, 683-690 (1998)
7. P. Mouroulis, D. A. Thomas, T. G. Chrien, V. Duval, R. O. Green, J. J. Simmonds, A.H. Vaughan, "Trade Studies in Multi/Hyperspectral Imaging Systems Final Report," in Jet Propulsion Laboratory files (29 October 1998)
8. R. B. Gomez, "Hyperspectral imaging: a useful technology for transportation analysis," in Optical Engineering 41, 2137-2143 (2002)

9. S. Jacquemond, S. L. Ustin, J. Verdebout, G. Schmuck, G. Andreoli, and B. Hosgood, "Estimating Leaf Biochemistry Using the PROSPECT Leaf Optical Properties Model," in *Remote Sensing of Environment*, Vol. 56, 194-202 (1996)
10. D. Schläpfer, "MODO: An Interface to MODTRAN for the Simulation of Imaging Spectrometry At-Sensor Signals," in *Summ. 10th Ann. JPL Airborne Earth Science Workshop Proc.*, JPL, Pasadena, pp. 8